Surface Characterization of Amorphous Aluminum Oxides

Sabine Goldberg,* Inmaculada Lebron, Donald L. Suarez, and Zeina R. Hinedi

ABSTRACT

Surface area is a physical property of solids that has been used as an indicator of reactivity and as an input parameter in chemical surface complexation models of ion adsorption. This study was conducted to identify the factors that affect the surface area of synthetic Al oxides and to evaluate whether surface area is a stable physical property of amorphous Al oxides. Four Al oxides were synthesized using four different methodologies. The surface area and porosity, especially mesoporosity, were characterized using gas adsorption, mercury intrusion porosimetry, scanning and transmission electron microscopy, and nuclear magnetic resonance (NMR) spectroscopy. Reactivity toward adsorption of borate, arsenite, arsenate, and molybdate as a function of solution pH, and ion activity products after aqueous reaction were also investigated. Surface areas were found to be affected by various factors, including aging, drying, heating, reaction in aqueous solution, and concentration of the starting reagents during synthesis. Aluminum oxide minerals of widely differing initial surface areas measured in the dry state had surface areas of comparable magnitude upon reaction in aqueous solution; the initially high surface areas decreased and the initially low surface areas increased to a surface area of 32.4 ± 2.8 $m^2 g^{-1}$. Initial surface area is not a good indicator of chemical reactivity for synthetic amorphous Al oxides. Accurate surface characterization is needed at the time of reaction if thermodynamically unstable materials are used in adsorption studies.

Due to their size, soil colloidal particles contain a large amount of reactive surface. Various soil physical and chemical properties, including ion adsorption capacity, are highly correlated with surface area. Amorphous particles are generally small in size, reactive, and have a large surface area. The predominant Al and Fe oxide phases in soils are often the amorphous species. These generally have larger surface area and greater reactivity toward anion adsorption than the corresponding crystalline mineral phases (Bohn et al., 1979). Because of their high reactivity, synthetic amorphous Al and Fe oxides are often studied as reference materials for the comparable amorphous minerals in soils that are difficult to isolate in pure form.

Surface area is a physical property of solids that has been used as an indicator of potential reactivity. Materials having higher surface area are considered to be more reactive in retention of nutrient ions and toxic trace elements. Surface area is also an important input parameter in chemical surface complexation models and transport models containing surface complexation models.

Surface areas of $>100\ m^2\ g^{-1}$ are expected for amorphous materials. Various synthesis methods have produced amorphous Al and Fe oxides exhibiting high reactivity toward ion adsorption suggestive of high surface area (Sims and Bingham, 1968; McPhail et al., 1972). These researchers did not characterize the surface area of these materials. In previous studies in our laboratory we obtained surface areas of $<15\ m^2\ g^{-1}$ for Al oxide and $>200\ m^2\ g^{-1}$ for Fe oxides using the synthesis methods of Sims and Bingham (1968), and $>200\ m^2\ g^{-1}$ for Al oxide using the preparation technique of McPhail et al. (1972). We attributed the differences in surface area of the Al oxides to differences in preparation method. Differences in surface area for synthetic oxides were also found by Schwertmann and Cornell (1991) for hematite, where a factor of two change in the concentration of one of the starting reagents resulted in an order of magnitude change in the surface area. Considerable differences in reactivity toward selenite adsorption were found for two goethites of similar surface area (Balistrieri and Chao, 1987; Hayes et al., 1988), which were probably due to differences in points of zero charge.

The objectives of our study were (i) to identify the factors that affect surface area of synthetic amorphous Al oxides, (ii) to evaluate whether surface area is a stable physical property of amorphous Al oxides, and (iii) to propose a synthesis methodology that produces amorphous Al oxides having surface areas consistent with their reactivity toward anion adsorption.

MATERIALS AND METHODS

Oxide Synthesis

Aluminum oxides were synthesized and freeze-dried using four different methodologies. The synthesis for the lowest surface area material was repeated and the product was split into two parts; one part was freeze-dried and the other was air-dried. In all methods, the $AlCl_3$/NaOH ratio was constant at a value of 0.375. Aluminum/OH ratio is a very important variable affecting the end product in Al oxide synthesis. Table 1 indicates the starting reagent concentrations for amorphous Al oxides of varying surface area. Using x-ray diffraction analysis, we found that all Al oxides were amorphous.

Characterization of Surface Area and Porosity

Specific surface areas were determined using both single-point and multipoint Brunauer–Emmett–Teller (BET) N_2 adsorption and desorption isotherms obtained with a Quantasorb Jr. Quantachrome surface area analyzer (Quantachrome, Syosset, NY).[1] Multipoint BET adsorption isotherms were conducted beginning at 5% and going to 95% N_2 and vice

Sabine Goldberg, Inmaculada Lebron, and Donald L. Suarez, USDA-ARS, U.S. Salinity Lab., 450 W. Big Springs Rd., Riverside, CA 92507; Zeina R. Hinedi, Dep. of Environmental Sciences, Univ. of California, Riverside, CA 92521. Contribution from the U.S. Salinity Lab. Received 8 Oct. 1999. *Corresponding author (sgoldberg@ussl.ars.usda.gov).

Published in Soil Sci. Soc. Am. J. 65:78–86 (2001).

[1] Trade names and company names are included for the benefit of the reader and do not imply any endorsement or preferential treatment of the product listed by the USDA.

Abbreviations: BET, Brunauer–Emmett–Teller; DDIW, doubly deionized water; EGME, ethylene glycol monoethyl ether; IAP, ion activity product; NMR, nuclear magnetic resonance; SEM, scanning electron microscope; TEM, transmission electron microscope.

Table 1. Starting reagents for synthesis of freeze-dried Al oxides.†

Surface area‡	$AlCl_3$ concentration	NaOH concentration	Supernatant solution pH	Reference
$m^2\ g^{-1}$	*M*			
13.05 ± 0.64	1.5	4.0	4.30	Sims and Bingham (1968)
74.7 ± 2.26	0.685	1.825	4.37	This study
140 ± 19.8	0.408	1.088	4.51	This study
239 ± 15.3	0.13	0.35	4.78	McPhail et al. (1972)

† $AlCl_3$/NaOH ratio is constant at 0.375. Reagents were reacted for 15 min prior to washing and freeze-drying the precipitates.
‡ Single-point Brunauer–Emmett–Teller N_2.

versa; multipoint BET desorption isotherms were conducted from 90 to 30% N_2. To determine multipoint BET surface areas 5 to 30% N_2 values were used. Ultrapure 100% N_2 and 100% He gases were mixed using Edwards High Vacuum International mass flow controllers (Edwards High Vacuum International, Crawley, UK) having a flow rate range of 0 to 50 standard $cm^3\ min^{-1}$. Additional specific surface area measurements were carried out using ethylene glycol monoethyl ether (EGME) adsorption (Cihacek and Bremner, 1979) and mercury intrusion porosimetry with a Quantachrome Poremaster 60 porosimeter. The mercury intrusion porosimetry measurements also provided pore-size distributions.

Single-point N_2 BET surface areas were determined as a function of temperature for the lowest and the highest initial surface area sample. Surface areas were determined after heating for 3 h to 100°C. Subsequently the same sample was heated for 3 h each at 200, 300, 400, 500, 600, 800, and 950°C followed by surface area determination.

We used NMR spectroscopy to determine the porosity of our samples (Hinedi et al., 1997). The Al oxides were packed into 5-mm-o.d. NMR tubes and saturated with water by capillary action. Longitudinal relaxation measurements of pore water were made on a JEOL FX200 NMR spectrometer (JEOL Inc., Peabody, MA) employing the inversion recovery pulse sequence (180°–*t*–90°) in which the delay time, *t*, varied between 0.25 and 5000 ms. More details about the interpretation of the relaxation time signals are provided in Hinedi et al. (1997).

Scanning and transmission electron microscopy were used to characterize the Al oxides obtained in the present study. The transmission electron microscope (TEM) was a Philips CM300 (Philips Analytical, Eindhoven, the Netherlands) operated at 300 kV accelerating voltage. The samples were deposited on copper grids coated with a thin holey carbon support film. Diffraction patterns of the samples were also observed in the TEM preparations. A scanning electron microscope (SEM) Philips XL30-FEG, operated at 20 kV was used to study the surface of the Al oxides, the samples were sputter-coated with Au–Pd alloy at a ratio of 60:40.

To quantify the particle size of the samples, thin sections of the Al oxides were prepared by impregnation of the samples with epoxy EPO-TEK 301 (Epoxy Technology Inc., Billerica, MA). After hardening, a 3.5 by 2.5 cm thin section was cut, mounted on a glass slide, and polished. In the polishing process, a series of diamond polishers was used to avoid introduction of contaminants; no water was present.

Thin sections were observed in a SEM (AMRAY, 3200, AM RAY Inc., Bedford, MA) using a backscatter electron detector. The intensity of the back-scattered electrons is a function of the atomic weight of the element, with heavier elements having higher back-scattering properties. Charging effects are counteracted by using low vacuum in the specimen chamber and by the introduction of air molecules to dissipate the charge accumulated on the surface of the sample. Sample coating is not needed. The quantification and classification of particle size and surface area were obtained using commercially available image analysis software (Princeton Gamma-Tech, Princeton, NJ).

Table 2. Surface areas of freeze-dried Al oxides using various techniques.

Surface areas			
Single point BET N_2†	Multipoint N_2 (5–30%)	Multipoint N_2 (30–5%)	Porosimetry
$m^2\ g^{-1}$			
12.6	7.4	7.3	4.8
76.3	40.8	41.0	38.9
126	64.8	65.6	49.2
254	145	147	101

† BET is Brunauer–Emmett–Teller.

Effect of Aging

Stability of the Al oxide phases was evaluated by equilibration in doubly deionized water (DDIW) at pH 4 and 5. These pH values were chosen so that experimentally detectable Al concentrations would be found in solution. Samples of oxide (0.3 g per 150 mL or 0.13 g per 25 mL) were added to 50-mL polypropylene centrifuge tubes or 250-mL centrifuge bottles and equilibrated to pH 4 or 5 with appropriate aliquots of DDIW (which had been preequilibrated to pH 4 or 5 using 1.0 *M* HCl). The samples were shaken for 2, 4, 8, 24, 120, or 216 h on a reciprocating shaker, centrifuged, analyzed for pH, and filtered through 0.1-μm cellulose nitrate filters. The filtrates were analyzed for Cl concentration using a chloride titrator and for Al concentration using the aluminon method described by Barnhisel and Bertsch (1982). Some of the remaining solids were air-dried and their N_2 BET surface area determined. The degree of aggregation and dispersion of the samples was evaluated visually after each shaking interval.

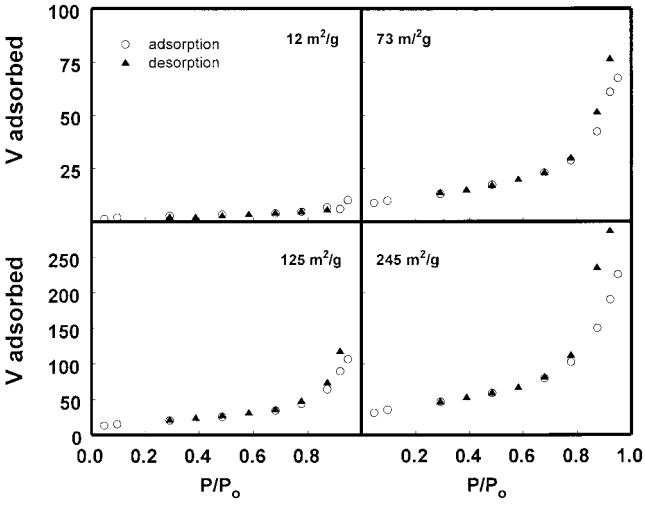

Fig. 1. Brunauer–Emmett–Teller N_2 adsorption–desorption isotherms for the initial Al oxide precipitates.

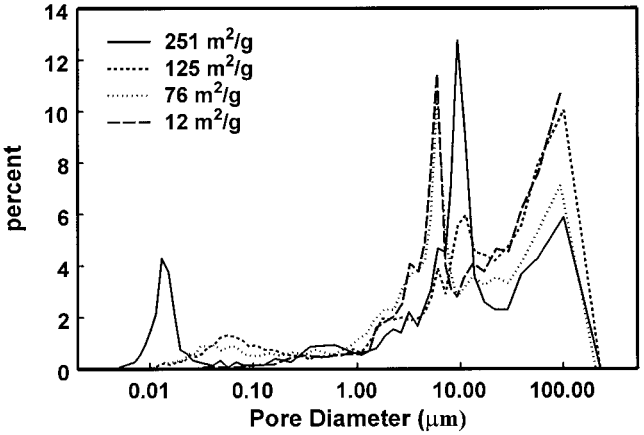

Fig. 2. Distribution of pore diameters obtained with mercury intrusion porosimetry for four amorphous Al oxides of different initial surface areas.

Ion activity products (IAPs) were calculated for each reaction interval.

Anion Adsorption Experiments

Anion adsorption experiments were carried out in batch systems to determine adsorption envelopes, amount of anion adsorbed as a function of solution pH per fixed total anion concentration for B, As, and Mo. Samples of oxide (0.078 g for B, 0.1 g for As, and 0.0525 g for Mo) were added to 50-mL polypropylene centrifuge tubes or 250-mL centrifuge bottles and equilibrated with aliquots (15 mL for B, 25 mL for arsenite, 200 mL for arsenate, and 150 mL for Mo) of a 0.1 *M* NaCl solution by shaking for 2 h on a reciprocating shaker. This solution contained 0.46 mmol L^{-1} B, 1.0 mmol L^{-1} As, or 0.29 mmol L^{-1} Mo and had been adjusted to the desired pH values using 1 *M* HCl or 1 *M* NaOH. Additions of acid or base changed the total volumes by <2%. After reaction, the samples were centrifuged and the decantates analyzed for pH, filtered using 0.45-μm cellulose nitrate filters, and analyzed for As and Mo concentration using inductively couple plasma emission spectrometry and B concentration using a Technicon Auto Analyzer II (Technicon Industrial Systems, Tarrytown, NY) and the Azomethine-H method (Bingham, 1982).

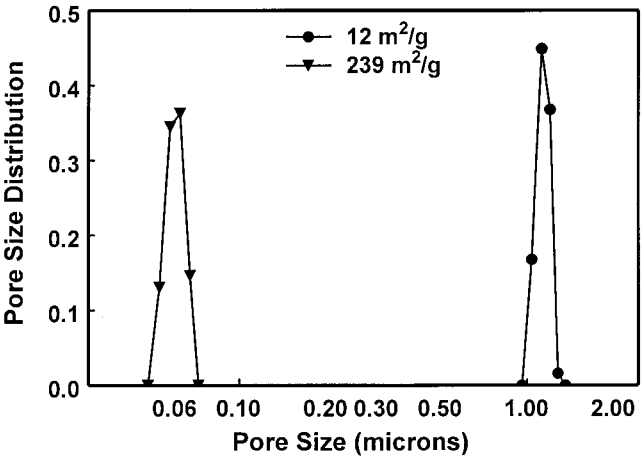

Fig. 3. Pore-size distribution obtained with nuclear magnetic resonance spectroscopy for two amorphous Al oxides of differing initial surface area.

Table 3. Dispersion behavior of Al oxides in doubly deionized water.

Reaction time	pH	Cloudy ⟵⟶ Clear
24 h	5	12 ≈ 76 > 126 > 254 m^2 g^{-1}
9 d	5	12 ≈ 76 ≈ 126 ≈ 254 m^2 g^{-1}
9 d	4	254 > 12 > 76 ≈ 126 m^2 g^{-1}

RESULTS AND DISCUSSION

Oxide Synthesis

Surface areas for four amorphous Al oxides synthesized using various methods are presented in Table 1. This information indicated that the surface area of amorphous Al oxide was very dependent on the concentrations of the starting reagents. An order of magnitude increase in the concentration of the starting reagents decreased the surface area of the product by a factor of 20. Increasing the concentration of the starting reagents greatly increased the product yield and usually increased the rate of precipitation as well.

Characterization of Surface Area and Porosity

Surface areas were determined with various experimental techniques as indicated in Table 2. Surface area is a relative measurement, whose values are scale dependent and dependent on measurement technique (Goldberg et al., 1999). This is due to the fractal nature of surface area; the smaller the scale of measurement, the larger the surface area value (Mandelbrot, 1983). For amorphous Al oxides it is especially important to understand the level of detail of the surface area characterization, since quantification of the internal porosity is expected to substantially affect the final surface area value and consequently our capability to understand the reactivity of these products. Surface areas of our samples for the different methods differed in value but trends were consistent. That is, the magnitude of the surface areas always exhibited the same order regardless of the method used. For example, EGME surface areas determined for these samples ranged from 222 to 425 m^2 g^{-1}. Examples of the reproducibility of the surface area measurements were 64.81 ± 0.85 m^2 g^{-1} for single-point BET N_2 adsorption and 232.6 ± 13.1 m^2 g^{-1} for EGME adsorption. The term *surface area* will be used to indicate single-point BET N_2 surface area unless otherwise specified.

Multipoint BET measurements were carried out using adsorption (5–95% N_2) and desorption (90–30% N_2) isotherms in order to evaluate hysteresis and thereby mesoporosity. Mesopores are defined as ranging in radius from 1 to 20 nm (Gregg and Singh, 1982). For the

Table 4. Single-point Brunauer–Emmett–Teller N_2 surface areas of freeze-dried Al oxides as affected by aging.

Surface areas	
Freeze-dried	Freeze-dried Aged 15 mo
m^2 g^{-1}	
12.6	7.8
76.3	57.0
126	69.2
254	139

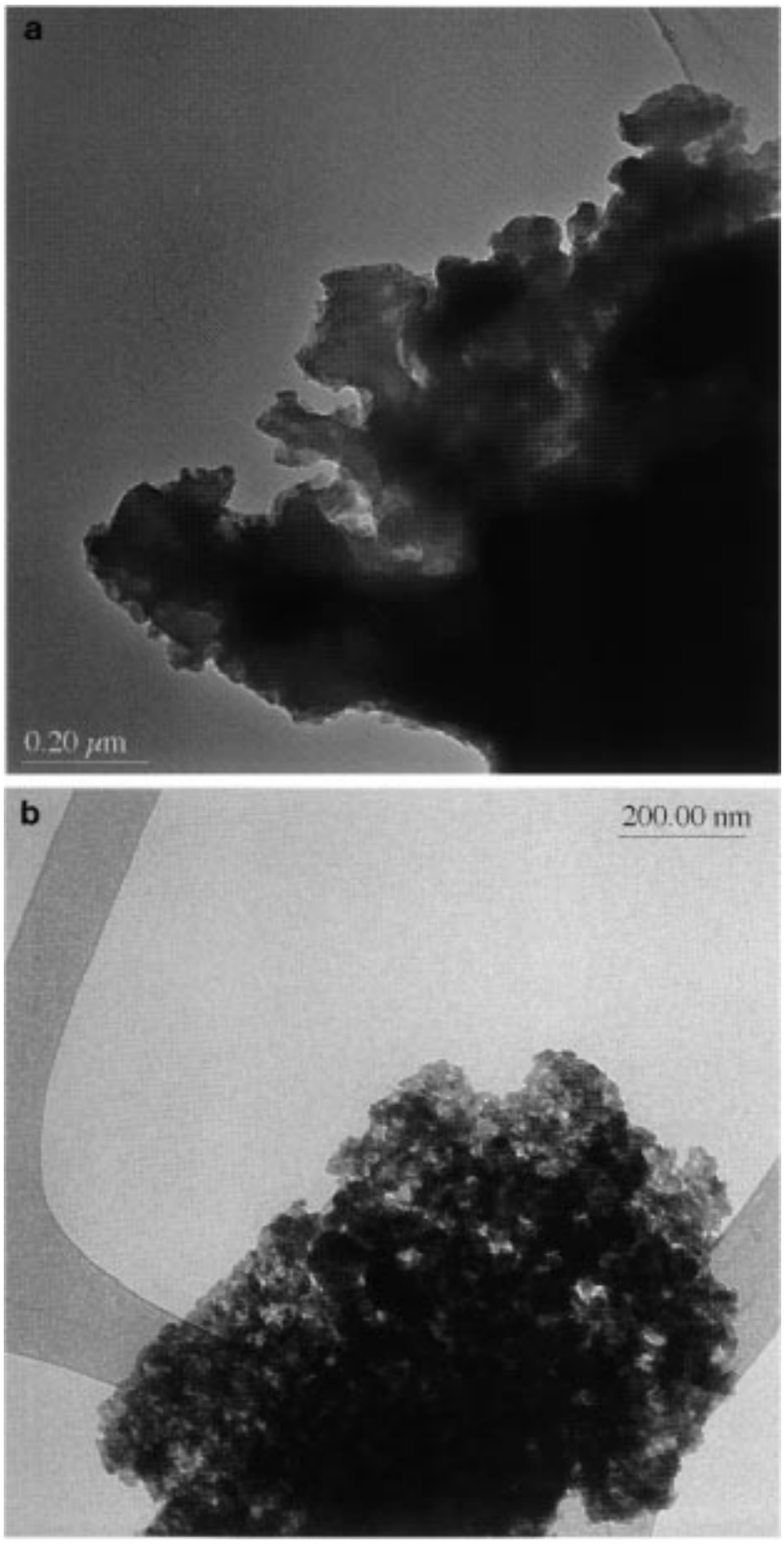

Fig. 4. Transmission electron micrographs showing Al oxide morphology. (a) Initial surface area: 12 $m^2 g^{-1}$, magnification: 14 500×; (b) initial surface area: 76 $m^2 g^{-1}$, magnification: 11 000×.

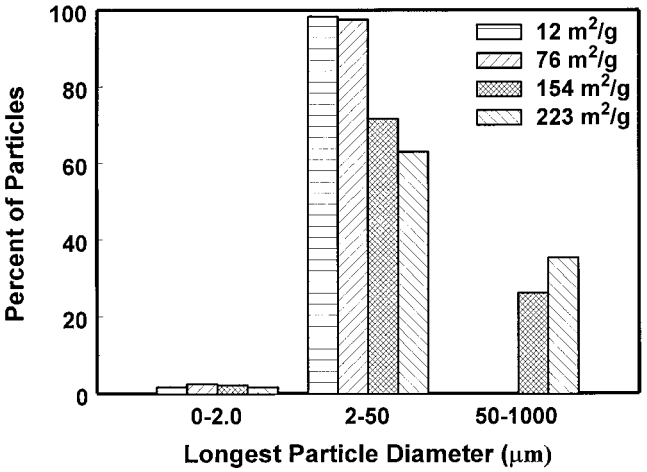

Fig. 5. Distribution of particle diameters obtained from scanning electron microscope measurements for four Al oxides of different initial surface areas.

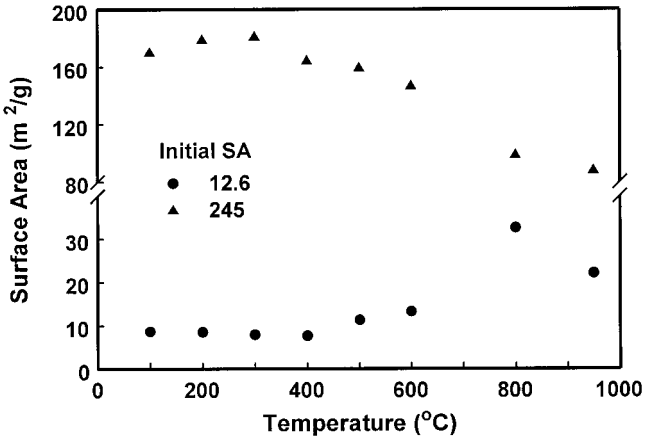

Fig. 6. Surface area as a function of temperature for two amorphous Al oxides of differing initial surface areas.

lowest surface area (12 $m^2\ g^{-1}$) sample, the adsorption and desorption isotherms were identical, indicating that no mesopores were present (Fig. 1). For the two intermediate surface areas, the isotherms started to deviate around 90% N_2, indicative of mesopores ≥9 nm. For the highest surface area (245 $m^2\ g^{-1}$) sample, the hysteresis commenced above 80%, N_2 indicative of mesopores ≥4 nm. For this high surface area material, there was significant hysteresis in the adsorption–desorption curves at 90 and 95% N_2. In accordance with the N_2 pressure–pore size relationships presented in Table 8.1 of Lowell and Shields (1991), hysteresis in this range corresponds to mesopores in the size range 9 to 19 nm. Pore sizes larger than 20 nm could not be determined as they occur in the relative pressure P/P_o range >0.95.

The mesoporosity of the highest surface area sample was confirmed by mercury intrusion porosimetry (Fig. 2) and by NMR (Fig. 3). Figure 2 indicates a population of pores around 13 nm in diameter for the highest surface area oxide, consistent with the N_2 measurements. Average pore size diameter for this sample was 60 nm obtained both with mercury intrusion porosimetry and NMR (Fig. 3). The mercury intrusion porosimeter method also showed a very small amount of mesoporosity for the two intermediate surface area Al oxides (Fig. 2). Average pore diameters obtained with mercury intrusion porosimetry were very similar in magnitude for all surface area materials.

Transmission electron micrographs (Fig. 4a and 4b) showed the morphology of the Al oxide particles. While the low surface area Al oxide particles were composed of large continuous particles (Fig. 4a); the other three samples contained particles that were conglomerates of smaller aggregates each ≈2 nm in length, as shown in Fig. 4b. These Al oxides were precipitated under various reagent concentrations. The low surface area Al oxide was precipitated in a much more concentrated environment resulting in very fast precipitation. In this situation, the double layer is very thin and primary particles can grow quickly and in a compact arrangement due to strong attractive forces. In contrast, when the double layer is more developed, repulsive forces dominate and dimers and longer chains organize into a card house structure with internal voids (Bagnall et al., 1990). This is seen as a composite of small crystals in the TEM pictures. The diffraction patterns of these composites did not show any significant crystalline organization.

The aggregation and dispersion behavior of suspended Al oxides was evaluated visually as the degree of cloudiness after various reaction times and is indicated in Table 3. After 24 h of reaction time at pH 5, the degree of cloudiness of the solution decreased with increasing surface area. That is, the highest surface area material had settled the most, indicating that this Al oxide contained the largest particles. Such an observation can only be consistent with high surface area if the particles are present as larger-size aggregates.

Quantification of particle sizes was performed by SEM measurements of thin sections prepared from Al oxide powders combined with image analysis techniques (Fig. 5). The methodology used to choose the appropriate magnification and the representativeness of the area sampled is described in Lebron et al. (1999). From Fig. 5 we can see that the Al oxides precipitated at the lower electrolyte concentration contained 26 to 35% of the particles >50 μm, while those precipitated at higher

Table 5. Dissolution of Al oxides in doubly deionized water at pH 5 for different reaction times (0.3 g per 150 mL).

Initial surface area†	2 h	4 h	8 h	1 d	5 d	9 d	9 day surface area
$m^2\ g^{-1}$	−log(IAP)‡			−log(IAP)			$m^2\ g^{-1}$
12.6	32.8	30.8	30.9	31.5	33.1	34.0	33.4
76.3	32.7	30.7	30.7	31.3	33.0	33.9	33.3
126	32.6	30.8	30.8	31.7	33.0	33.8	34.7
254	32.4	31.3	31.2	31.8	33.0	33.5	28.3

† Single-point Brunauer–Emmett–Teller N_2.
‡ IAP is ion activity product.

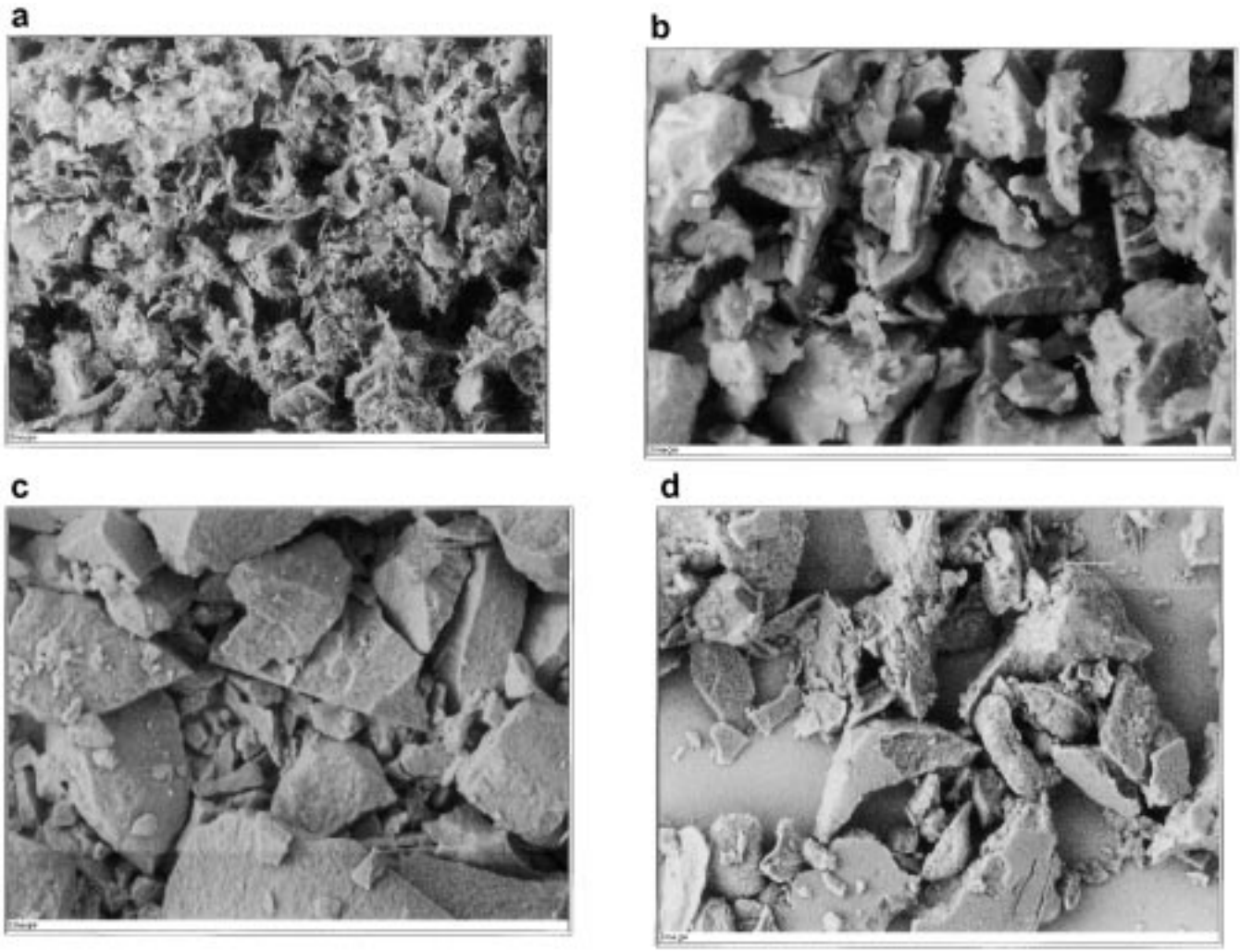

Fig. 7. Scanning electron micrographs showing Al oxide morphology (a, b) before and (c, d) after suspension in water for 9 d: (a, c) lowest initial surface area; (b, d) highest initial surface area.

electrolyte concentration consisted of particles in the size range of 2 to 50 μm.

Effect of Aging

Surface area of these Al oxide minerals was not only dependent on preparation but was also affected by aging time and treatment. We split a newly synthesized batch of the low surface area Al oxide, freeze-drying one half and allowing the other half to air-dry. The single-point BET N_2 surface area of the freeze-dried subsample was 28.0 $m^2\ g^{-1}$, while that of the air-dried subsample was 5.0 $m^2\ g^{-1}$. Freeze-drying may produce a different pore structure than air-drying. As will be shown below, the reactivity toward anion adsorption of these two subsamples was also different.

Surface area changes due to heating to various temperatures are indicated in Fig. 6. Surface area of the sample initially at 12.6 $m^2\ g^{-1}$ increased by a factor of three when heated to 800°C, while surface area of the sample initially at 245 $m^2\ g^{-1}$ decreased by a factor of two following heating above 800°C. These observations suggest that the materials are transforming and recrystallizing into a relatively more thermodynamically stable structure. Similar results for an anomalously low surface area silica-alumina gel were found by Hietela et al. (1989, 1990). These authors interpreted the increase in surface area with increasing temperature of the low surface area material as partially closed porosity. They hypothesized that their low surface area material possesses a fraction of pores that are closed at low temperature and therefore do not contribute to the measured surface area. Upon heating to high temperature these pores open and their surface area becomes measurable.

Freeze-dried Al oxides aged in plastic sample containers for 15 mo exhibited significantly reduced surface

Table 6. Dissolution of Al oxides in doubly deionized water at pH 5 (0.13 g per 25 mL) for two reaction times.

Initial surface area†	Final surface area† 24-h reaction	2-h reaction	24-h reaction
$m^2\ g^{-1}$		−log(IAP)‡	−log(IAP)
12.6	89.7	30.9	30.3
73.1	101	30.8	30.6
126	98.8	30.3	30.2
245	137	30.8	31.0

† Single-point Brunauer–Emmett–Teller N_2.
‡ IAP is ion activity product.

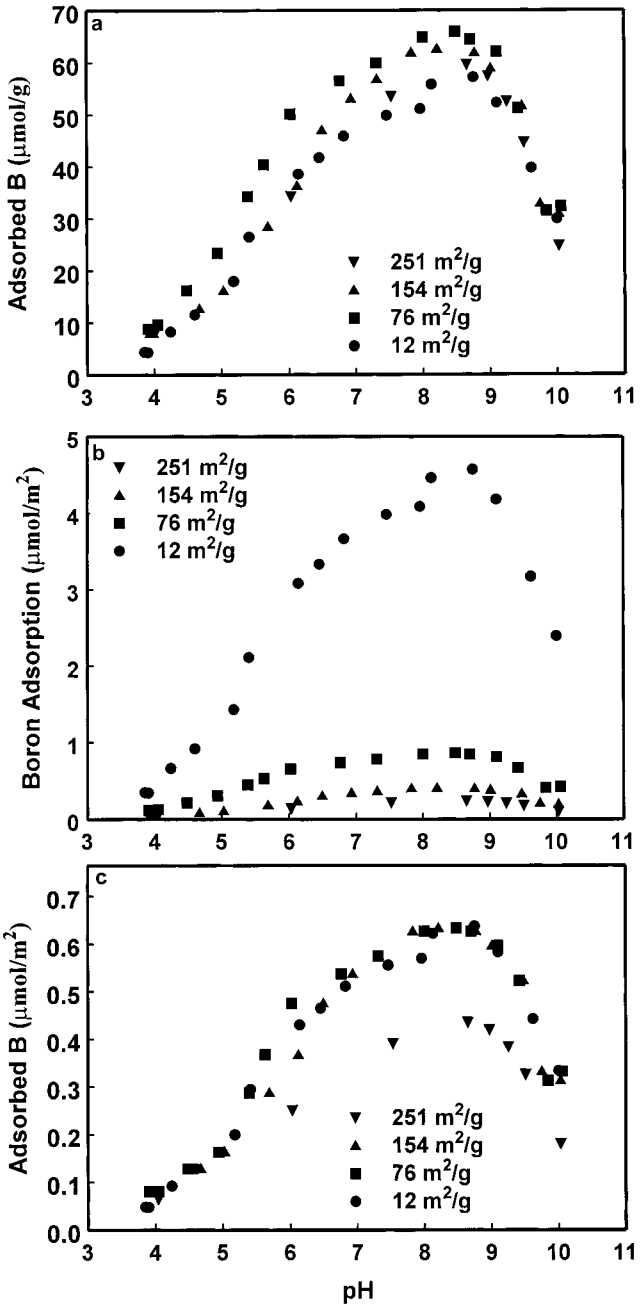

Fig. 8. Boron adsorption as a function of solution pH for four amorphous Al oxides of differing initial surface areas expressed on a: (a) per gram basis, (b) per meter squared of initial surface area basis, (c) per meter squared of final surface area basis.

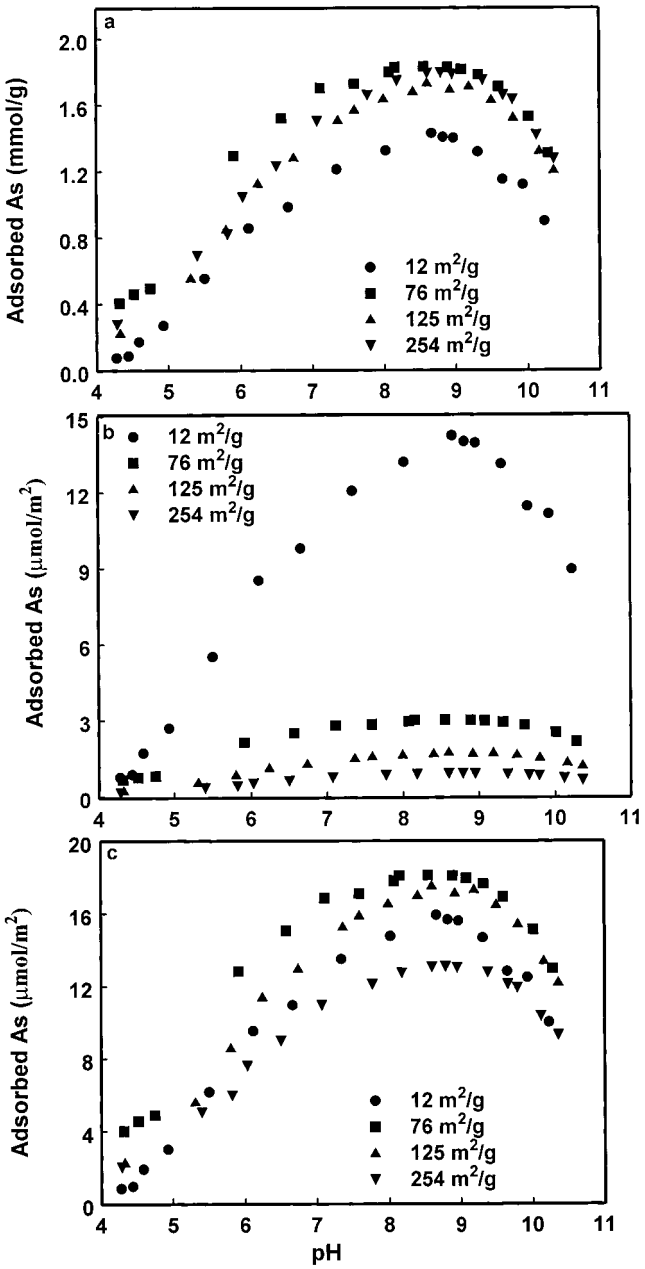

Fig. 9. Arsenite adsorption as a function of solution pH for four amorphous Al oxides of differing initial surface areas expressed on a: (a) per gram basis, (b) per meter squared of initial surface area basis, (c) per meter squared of final surface area basis.

areas as shown in Table 4. Aging has also been found to decrease the surface area of goethite and hematite (Diakonov et al., 1994). The instability of these surface area values draws into question the use of initial surface area as a parameter in chemical characterization of these amorphous oxides.

Scanning electron micrographs were obtained for the original Al oxide precipitates and the products after 9 d of reaction in water on unground air-dried material. Figure 7 shows the micrographs for the Al oxides having the lowest (Fig. 7a and 7c) and the highest surface area (Fig. 7b and 7d). Figures 7a and 7b show the original oxides, while Fig. 7c and 7d show these oxides after aging for 9 d. The original lowest surface area material (Fig. 7a) contains not only smaller particles, as previously quantified in the equivalent preparation in thin sections (Fig. 4a), but also exhibits a flake-like texture in agreement with a poorly organized structure. The original highest surface area material (Fig. 7b) exhibits much bigger particles with better defined edges than in Fig. 7a, showing a more consolidated material with a conchoidal fracture. After 9 d of aging in water, both the lowest and highest surface area oxides appear very similar, with an angular fracture pattern consistent with the more crystalline structure evidenced by the x-ray diffraction results discussed below.

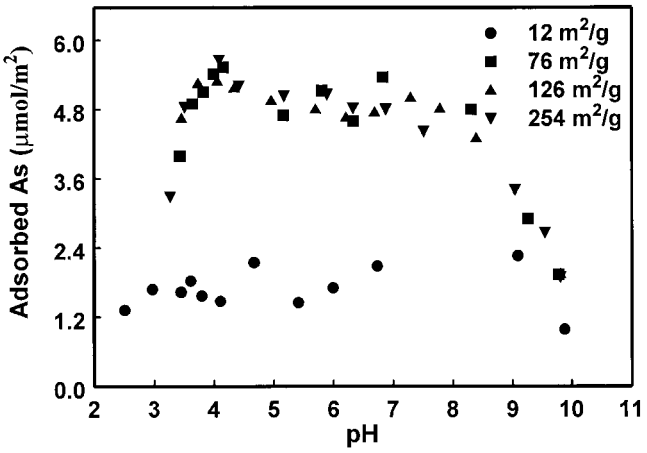

Fig. 10. Arsenate adsorption as a function of solution pH for four amorphous Al oxides of differing initial surface areas expressed on a per meter squared of final surface area basis.

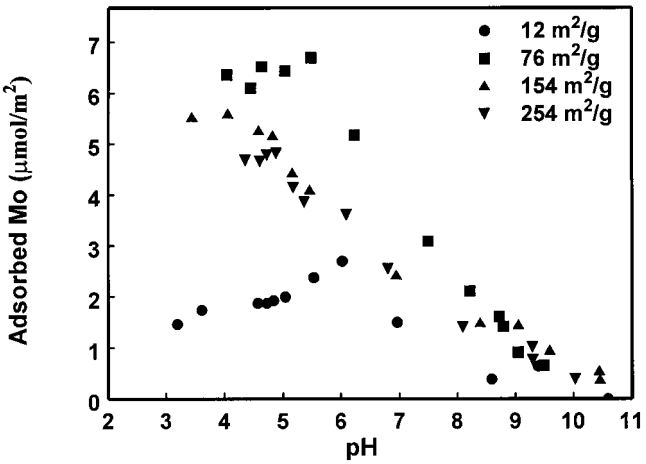

Fig. 11. Molybdate adsorption as a function of solution pH for four amorphous Al oxides of differing initial surface areas expressed on a per meter squared of final surface area basis.

Aluminum oxides suspended in water for 24 h showed different degrees of cloudiness due to different size aggregates, as indicated above. After 9 d of reaction time, some of these aggregates had apparently separated, since the turbidity of all surface area materials was now the same. After 9 d of treatment at the more aggressive pH 4 dissolution treatment, all aggregates had apparently broken down, since the highest surface area material yielded the cloudiest solution and thus presumably contained the smallest size particles, consistent with its high surface area.

Ion activity products indicated in Tables 5 and 6 were calculated for all Al oxides after various periods of reaction time using the chemical speciation program WATEQ4F (Ball and Nordstrom, 1991). At reaction times <1 d, the log(IAP) values compared favorably with the $\log K_{so} = -31.1$ value for amorphous Al oxide (Ball and Nordstrom, 1991). At the longest reaction time of 9 d, the calculated log(IAP) values (−33.5 to −34.0) were intermediate between the solubility of amorphous Al oxide and gibbsite ($\log K_{so} = -35.0$; Ball and Nordstrom, 1991). X-ray diffraction analyses verified the presence of gibbsite after 9 d of reaction. These results indicated that the amorphous Al oxides were unstable relative to gibbsite and were dissolving and recrystallizing into the more stable solid phase with time. However, independent of initial conditions, the log(IAP) values for the four different surface area Al oxides did not show significant differences. Thus their differing initial surface areas were not due to differences in the type of solid Al phase.

Surface areas after aging, obtained for the Al oxides having diverse initial surface areas, are presented in Tables 5 and 6. The final surface areas of the samples reacted for 24 h were converging on a value, 107 ± 21 $m^2\ g^{-1}$. This observation is especially remarkable because the lowest surface area sample was increasing from 12.6 to 89.7 $m^2\ g^{-1}$, while the highest surface area sample was decreasing from 245 to 137 $m^2\ g^{-1}$. It appears that upon reaction in aqueous solution, these Al oxides, despite differing initial surface areas, measured in the dry state, act as the same solid phase having the identical log(IAP) value and comparable surface area in solution.

Reaction of the amorphous Al oxides for 9 d in aqueous solution at pH 5 yielded surface areas of 32.4 ± 2.8 $m^2\ g^{-1}$. These surface areas were effectively replicates of each other, indicating that the Al oxides had transformed toward the same solid phase.

Adsorption Experiments

Adsorption envelopes for the adsorption of various anions are depicted in Fig. 8 through 12. Borate (Fig. 8) and arsenite (Fig. 9) adsorption exhibited parabolic behavior, with adsorption increasing with increasing solution pH up to an adsorption maximum near pH 9. Adsorption decreases as solution pH continues to increase. These results are in agreement with previous results obtained for B (Goldberg and Glaubig, 1985) and arsenite (Manning and Goldberg, 1997) adsorption on amorphous Al oxide. Borate and arsenite adsorption envelopes on all four Al oxides were very similar in magnitude on a per gram basis (Fig. 8a and 9a) despite initial surface areas differing by a factor of 20. Expression of the data on an initial surface area basis (Fig. 8b and 9b) suggests that the 12 $m^2\ g^{-1}$ material is very

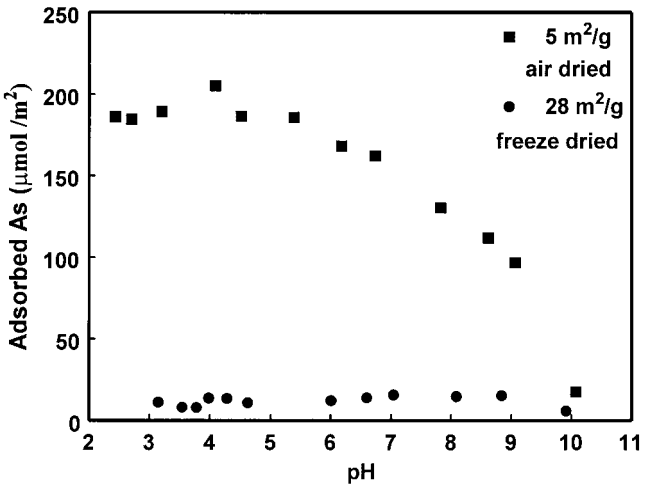

Fig. 12. Arsenate adsorption as a function of solution pH and method of drying for two amorphous Al oxides of differing initial surface areas.

reactive and appears to adsorb out of proportion to its measured surface area. Expression of the data on a final surface area basis following aqueous reaction (Fig. 8c and 9c) indicates that all four materials have similar reactivity. This is not surprising since the final surface area of all materials was in the same order of magnitude.

Arsenate and molybdate exhibited similar adsorption behavior (Fig. 10 and 11). Adsorption as a function of solution pH was maximum at a pH value between 4 and 5 and decreased as solution pH continued to increase. These results are in agreement with previous results obtained for arsenate (Anderson et al., 1976) and molybdate (Goldberg et al., 1996) adsorption on amorphous Al oxide. For both of these ions, adsorption was similar in magnitude for the three highest surface areas. The lowest surface area oxide exhibited the lowest adsorption on a per gram basis and the highest adsorption on an initial surface area basis (data not shown). On a final surface area basis, the lowest surface area showed the lowest adsorption (Fig. 10 and 11). It is possible that the presence of the arsenate and molybdate ions interfered with the surface transformations so that the surface areas in the presence of the anions may not be the same as in their absence. These results suggest that surface area measurements on freshly made, freeze-dried solids may provide misleading conclusions as regards anion reactivity. Surface areas measured after reaction in aqueous solution are much more appropriate for deducing reactivity of amorphous Al oxide minerals.

Figure 12 compares the reactivity of freeze-dried vs. air-dried Al oxide toward arsenate adsorption. On an initial surface area basis, the air-dried amorphous oxide was about 20 times more reactive than the freeze-dried oxide. This result suggests that surface area is sensitively dependent on treatment conditions.

CONCLUSIONS

The observation that Al oxide minerals having widely differing initial surface areas measured in the dry state attained comparable surface area upon reaction in solution casts doubt on the use of initial BET surface areas as chemical characterization parameters indicative of mineral reactivity. Presently it is our recommendation that surface areas of synthetic amorphous Al oxides be determined after reaction in aqueous solution in order to have applicability to understanding adsorption reactions. We recommend starting reagent concentrations of $AlCl_3$ of 0.408 to 0.685 *M*, NaOH of 1.088 to 1.825 *M*, and $AlCl_3$/NaOH ratio of 0.375, as these materials showed the smallest surface area changes between the initial and reacted surface areas. We believe that our results may have applicability to other amorphous minerals, especially Fe oxides, and evaluation of these systems is warranted.

ACKNOWLEDGMENTS

Gratitude is expressed to Mr. H.S. Forster, Mr. C. Bennett, and Ms. M. Scott for technical assistance.

REFERENCES

Anderson, M.A., J.F. Ferguson, and J. Gavis. 1976. Arsenate adsorption on amorphous aluminum hydroxide. J. Colloid Interface Sci. 54:391–399.

Bagnall, C.M., L.G. Howarth, and P.F. James. 1990. Modeling of aggregation kinetics of colloidal silica particles. J. Non-Crystalline Solids 121:56–60.

Balistrieri, L.S., and T.T. Chao. 1987. Selenium adsorption on goethite. Soil Sci. Soc. Am. J. 51:1145–1151.

Ball, J.W., and D.K. Nordstrom. 1991. User's manual for WATEQ4F, with revised thermodynamic data base and test cases for calculating speciation of major, trace, and redox elements in natural waters: U.S. Geological Survey Open-File Rep. 91-183. U.S. Geological Survey, Reston, VA.

Barnhisel, R., and P.M. Bertsch. 1982. Aluminum. p. 275–300. *In* A.L. Page et al. (ed.) Methods of soil analysis. Part 2. Agron. Monogr. 9. ASA and SSSA, Madison, WI.

Bingham, F.T. 1982. Boron. p. 431–447. *In* A.L. Page et al. (ed.) Methods of soil analysis. Part 2. Agron. Monogr. 9. ASA and SSSA, Madison, WI.

Bohn, H.L., B.L. McNeal, and G.A. O'Connor. 1979. Soil chemistry. John Wiley & Sons, New York.

Cihacek, L.J., and J.M. Bremner. 1979. A simplified ethylene glycol monoethyl ether procedure for assessment of soil surface area. Soil Sci. Soc. Am. J. 43:821–822.

Diakonov, I., I. Khodakovsky, J. Schott, and E. Sergeeva. 1994. Thermodynamic properties of iron oxides and hydroxides. I. Surface and bulk thermodynamic properties of goethite (α-FeOOH) up to 500 K. Eur. J. Mineral. 6:967–983.

Goldberg, S., and R.A. Glaubig. 1985. Boron adsorption on aluminum and iron oxide minerals. Soil Sci. Soc. Am. J. 49:1374–1379.

Goldberg, S., H.S. Forster, and C.L. Godfrey. 1996. Molybdenum adsorption on oxides, clay minerals, and soils. Soil Sci. Soc. Am. J. 60:425–432.

Goldberg, S., I. Lebron, and D.L. Suarez. 1999. Soil colloidal behavior. p. B195–240. *In* M.E. Sumner (ed.) Handbook of soil science. CRC Press, Boca Raton, FL.

Gregg, S.J., and K.S.W. Singh. 1982. Adsorption, surface area and porosity. Academic Press, London.

Hayes, K.F., C. Papelis, and J.O. Leckie. 1988. Modeling ionic strength effects on anion adsorption at hydrous oxide/solution interfaces. J. Colloid Interface Sci. 125:717–726.

Hietala, S.L., D.M. Smith, J.L. Golden, and C.J. Brinker. 1989. Anomalously low surface area and density in the silica-alumina gel system. J. Am. Ceram. Soc. 72:2354–2358.

Hietala, S.L., D.M. Smith, C.J. Brinker, A.J. Hurd, A.H. Carim, and N. Dando. 1990. Structural studies of anomalous behavior in the silica-alumina gel system. J. Am. Ceram. Soc. 73:2815–2821.

Hinedi, Z.R., A.C. Chang, M.A. Anderson, and D.B. Borchardt. 1997. Quantification of microporosity by NMR relaxation of water imbibed in porous media. Water Resour. Res. 33:2697–2704.

Lebron, I., M.G. Schaap, and D.L. Suarez. 1999. Saturated hydraulic conductivity prediction from microscopic pore geometry measurements and neural network analysis. Water Resour. Res. 35: 3149–3158.

Lowell, S., and J.E. Shields. 1991. Powder surface area and porosity. Chapman & Hall, London.

Mandelbrot, B.B. 1983. The fractal geometry of nature. Freeman and Co., New York.

Manning, B.A., and S. Goldberg. 1997. Adsorption and stability of arsenic(III) at the clay mineral–water interface. Environ. Sci. Technol. 31:2005–2011.

McPhail, M., A.L. Page, and F.T. Bingham. 1972. Adsorption interactions of monosilicic and boric acid on hydrous oxides of iron and aluminum. Soil Sci. Soc. Am. Proc. 36:510–514.

Schwertmann, U., and R.M. Cornell. 1991. Iron oxides in the laboratory. Preparation and characterization. VCH Publ., New York.

Sims, J.T., and F.T. Bingham. 1968. Retention of boron by layer silicates, sesquioxides, and soil materials: II. Sesquioxides. Soil Sci. Soc. Am. Proc. 32:364–369.